Bacteriophage Viruses as Confined Liquid Crystals

M. Carme Calderer

School of Mathematics
University of Minnesota

Conference on Variational Models of Soft Matter
Facultad de Matemáticas
Pontificia Universidad Católica de Chile

January 9-13 , 2017

Abstract

Folding of viral DNA in a capsid yields a highly ordered liquid crystal phase, with a disordered inner region, subject to extreme pressures, about 60 atmospheres.
This is due to two main properties of the DNA molecule:

- high bending resistance,
- large negative charge chirally arranged along the axis.

We assume that the DNA inside the capsid is a lyotropic liquid crystal hydrogel, with DNA embedded in environmental water that sustains ions.
The LC is a biaxial smectic A realized by an elastomer filament.
LC defects, points and dislocations, are associated with filament crossings and knots.

Outline

- Mechanical Modeling. Energy
  - Biaxial smectic A liquid crystal
  - Indexing layer locations
  - Reconstituting the elastic filament
- Determining material parameters
- Free boundary problems
- DNA hydrogel
- Conclusions

Joint work with Javier Arsuaga and Mariel Vázquez. Graduate students: Lindsey Hiltner (Minnesota), Tamara Christiani (Davis).

Data

We present a liquid crystal based model of DNA packing inside a capsid. The data at our disposal include:

- cryongenic images
  - density graphs
  - capsid shape and core
  - size of disordered region
- DNA effective diameter and genome length
- DNA concentration inside capsid
- pressure measurements
- DNA ejection force and speed.

Background on smectic A liquid crystals

director $\boldsymbol{n}$, complex order parameter $\psi = \rho e^{iq\omega}$.

$$\mathcal{E}_{\mathrm{A}} = \int_{\Omega} \left(F_{\mathrm{N}}(\nabla \boldsymbol{n}, \boldsymbol{n}) + F_{\mathrm{Sm}}(\nabla\psi, \psi, \boldsymbol{n}) \right) d\mathbf{x},$$

$$F_{\mathrm{Sm}} = C_{\parallel} |\nabla\psi - iq\boldsymbol{n}|^2 + f(|\psi|)$$

$$|\nabla\psi - iq\boldsymbol{n}|^2 = \rho^2 |\nabla\omega - q\boldsymbol{n}|^2 + |\nabla\rho|^2$$

$$F_N = K_1(\nabla \cdot \boldsymbol{n})^2 + K_2(\boldsymbol{n} \cdot \nabla \times \boldsymbol{n} + \tau)^2 + K_3 |\boldsymbol{n} \times (\nabla \times \boldsymbol{n})|^2$$

$$+ (K_2 + K_4)(\mathrm{tr}\,(\nabla \boldsymbol{n})^2 - (\nabla \cdot \boldsymbol{n})^2)$$

Interlayer spacing $d = \frac{2\pi}{q}$

[Lubensky, Renn; 1988, 1990].

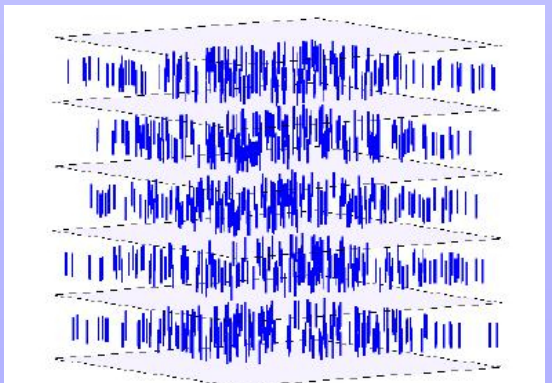

Existence of minimizer of chiral smectic A energy for weak and strong anchoring shown in [Bauman, MCC, Liu, Phillips; 2002]. Phase transition from nematic to smectic A shown as K_2 diverges.

Smectic A density graph

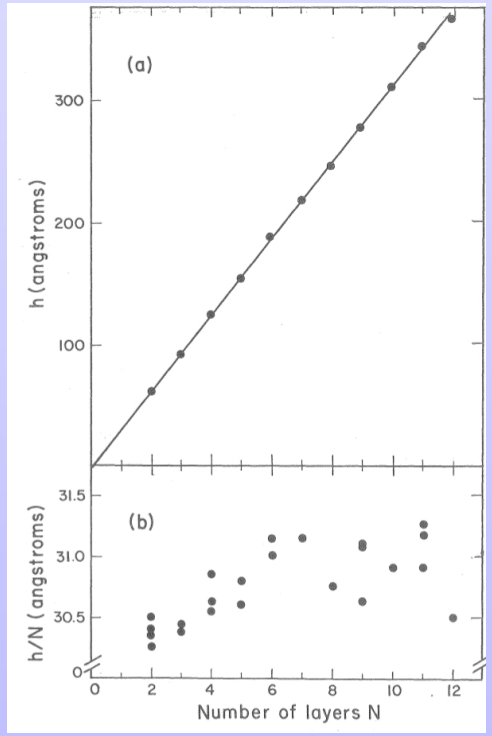

Optical measurements of smectic A layer spacing in freely suspended thin films [Rosenblatt and Amer, 1979]. The number of layers $2 \leq N \leq 15$. Use of optical interference techniques to measure interlayer spacing; films are much thinner than optical wavelengths.

Number of layers similar to that in the ordered region of the capsid.

Density graphs

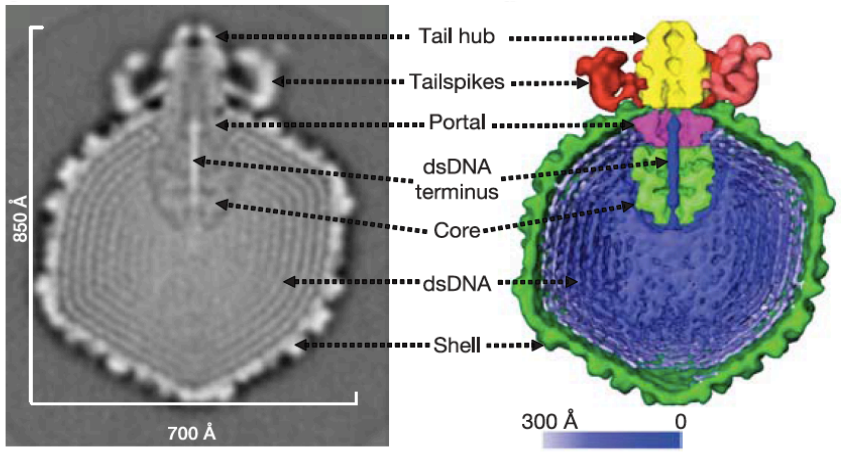

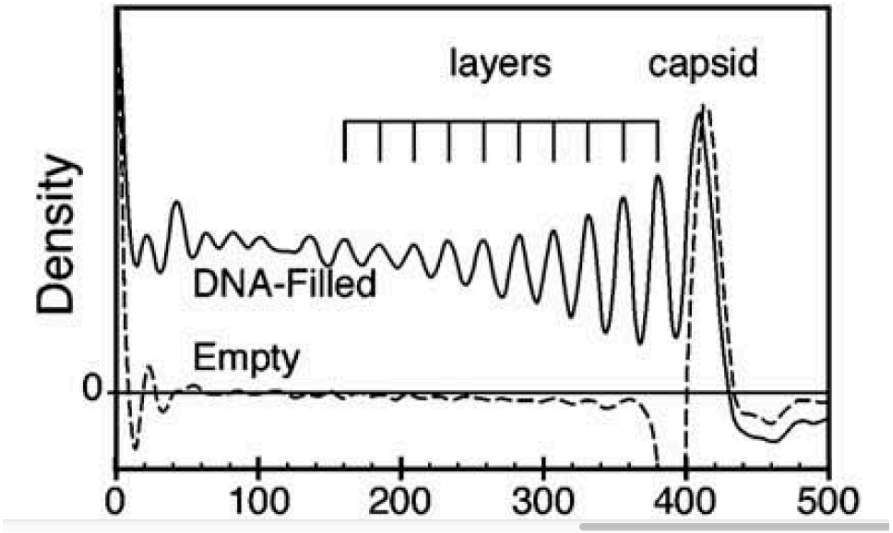

Chromonic liquid crystal shapes

Molecules have disc-like shape that stack into columns and higher superstructures. Form nematic and columnar phases. DNA has been described as chromonic liquid crystal with base pairs arranged along a central filament axis. A main difference between chromonic structures and DNA capsids is that the latter sustains pressures of several order of magnitude of the chromonic ones. Both systmes share a bending resistance property and affinity for water.

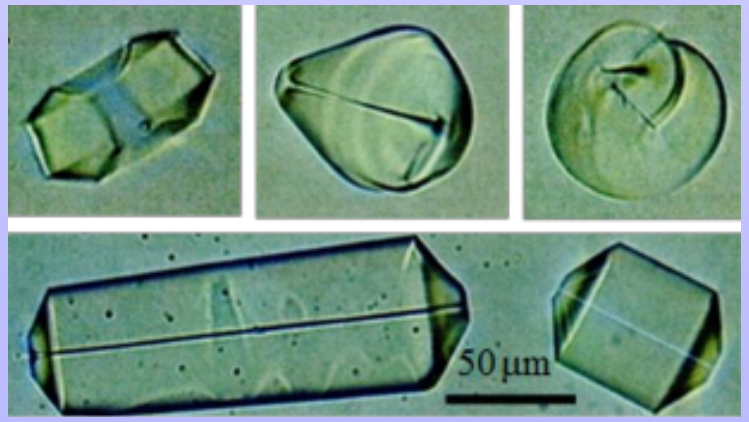

Kumar, Lavrentovich (2010).
Picuture kindly lent by O. Lavrentovich.

Nematic and biaxial smectic A vector fields

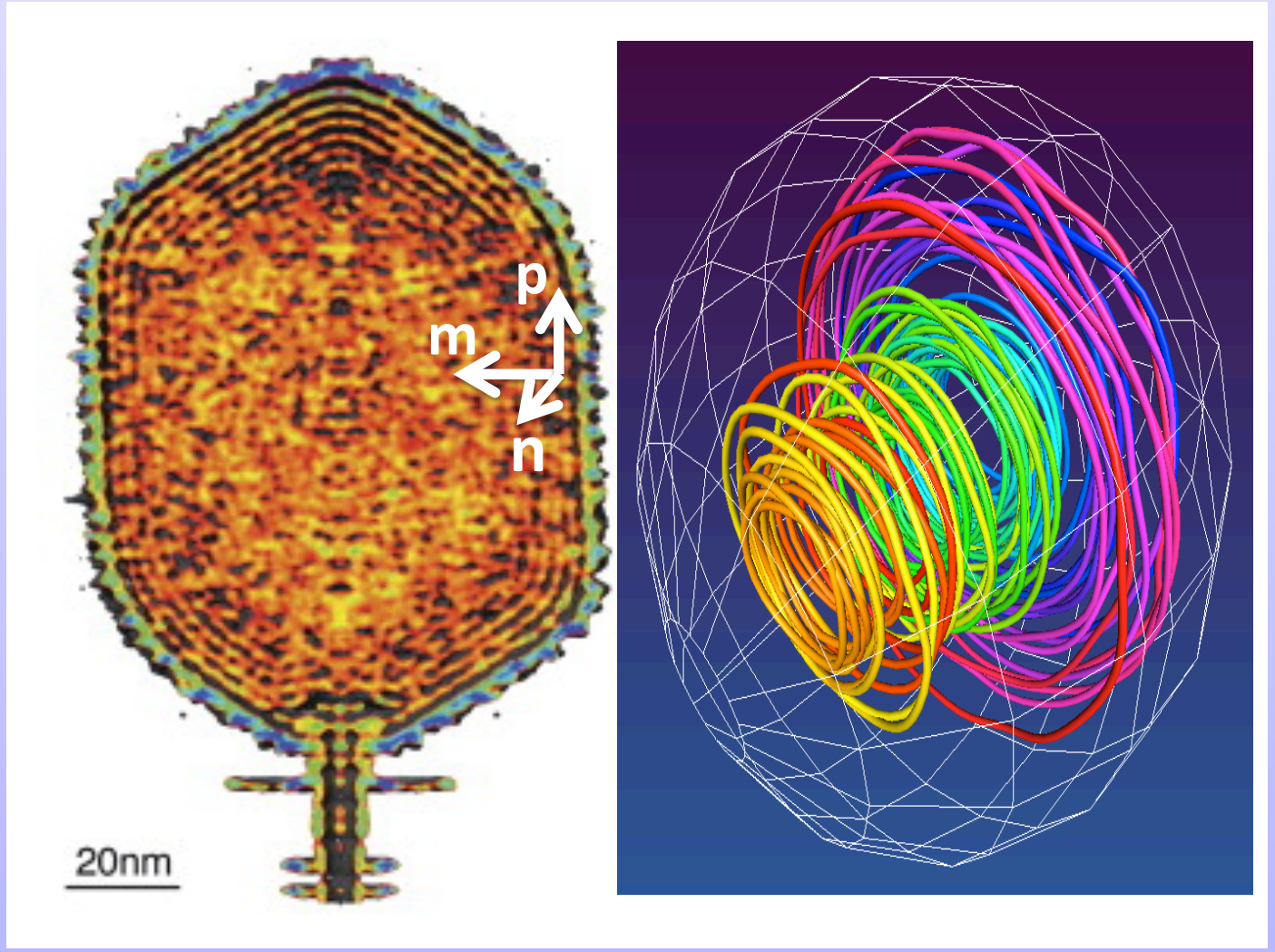

Variable fields and unknowns of the model

- $\boldsymbol{n}$: unit nematic director. Local tangent vector to the filament.
- $\boldsymbol{m}$, ψ: meridian layer direction and smectic density.
- $\boldsymbol{p}$, γ: parallel layer direction and smectic density.

$$\psi = \rho e^{iq\omega}, \;\; \gamma = \rho e^{iq\vartheta}$$
$$|\mathbf{m}| = 1, \, |\boldsymbol{n}| = 1, \, |\boldsymbol{p}| = 1.$$

- Interlayer distance $d = \frac{2\pi}{q}$: effective DNA diameter.
- Discrete families of level surfaces

$$\{\mathcal{S}^i_{\mathbf{m}}\}_{i=1}^{M} : \omega(\mathbf{x}) = m_i$$
$$\{\mathcal{S}^j_{\boldsymbol{p}}\}_{j=1}^{P} : \vartheta(\mathbf{x}) = p_j$$

$\diamond$ Smectic layers provide skeleton for DNA organization and space filling mechanism.

Level surfaces

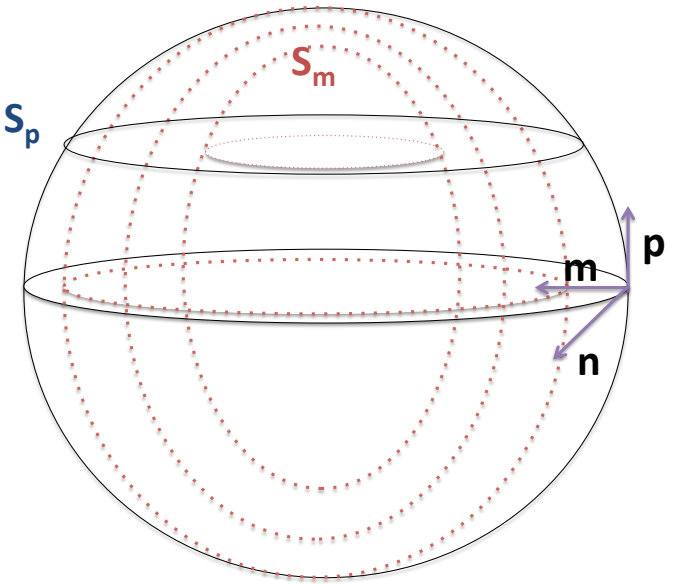

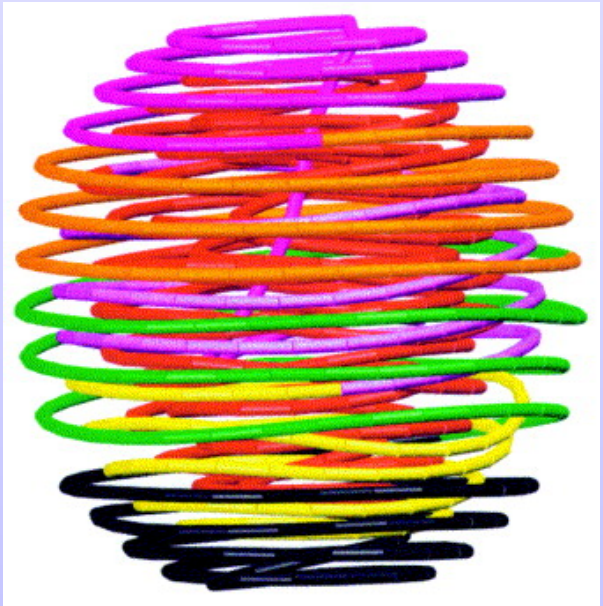

$$\{\mathcal{S}^i_{\mathbf{m}}\}_{i=1}^{M} : \omega(\mathbf{x}) = m_i$$

$$\{\mathcal{S}^j_{\boldsymbol{p}}\}_{j=1}^{P} : \vartheta(\mathbf{x}) = p_j$$

DNA filament will occupy level curves intersecting level surfaces of both families: $\mathcal{S}^i_{\mathbf{m}} \cap \mathcal{S}^j_{\boldsymbol{p}}$

Bacteriophage Virus Energy

$\Omega \subset \mathcal{B}$: ordered region inside capsid. Unknown.
$\Omega_0 \subset \mathcal{B}$: disordered region. $\mathcal{B} = \Omega \cup \Omega_0$.

$$
\begin{aligned}
F_{AN} =& F_N(\nabla \boldsymbol{n}, \boldsymbol{n}) + F_N(\nabla \mathbf{m}, \mathbf{m}) + F_N(\nabla \boldsymbol{p}, \boldsymbol{p}) \\
&+ C_s\left(|\nabla\psi - iq\psi \boldsymbol{p}|^2 + |\nabla\gamma - iq\gamma \mathbf{m}|^2\right) \\
&+ A(\mathbf{m}\cdot\boldsymbol{n})^2 + B(\mathbf{m}\cdot\boldsymbol{p})^2 + C(\boldsymbol{n}\cdot\boldsymbol{p})^2, \\
E =& \int_\Omega F_{AN}\, d\mathbf{x} + \nu \mathrm{Vol}(\Omega_0) + \sigma \mathrm{Area}(\partial\Omega_0).
\end{aligned}
$$

- ν, energy density of isotropic phase.
- σ, surface energy density of ordered/disordered interface.
- $A, B, C \gg 1$ ensure orthogonality in packing
- $B = \frac{1}{\epsilon^2} + \epsilon p_G(z)$, Gaussian random noise to account for departure from *perfect* packing.

Model Assumptions I

- As for semiflexible polymers, assume that

$$K_3 = \frac{K_B T L_p}{I}.$$

  L_p persistence length of the DNA, it takes values between 20 to 200 nm;

  I geometric moment of inertia of the ordered structure with respect to the capsid axis. Note that I is a function of the distance to the capsid axis, so, K_3 accounts for the increase in bending resistance as the axis is approached.

- From recent work on chromonic liquid crystals by Lavrentovich and Zhou (Ph.D thesis, Liquid Crystals Institute, May 2016): $K_1 \approx K_3 \approx 10K_2$.

Model Assumptions II

- Observations that viral genome occupies the whole capsid:

$$C_S = C_S(c),\ C_S(0) = 0,\ C_S'(c) > 0,\ \lim_{c \to 1^-} C_S(c) = +\infty$$

- Also,

$$\nu = \nu(c),\ \nu'(c) > 0;\ \sigma = \sigma(c), \sigma'(c) > 0$$

Take expressions for lyotropic liquid crystals by Onsager[1949] and Doi [1983-84].
Num. studies of DNA concentration in different capsids Purohit [2005].

Boundary conditions: capsid surface is the first p-Level Surface

The role of the capsid proteins in promoting filament ordering dictates the choice of boundary conditions of the problem.

- Assume capside be a smooth axisymmetric surface $\mathcal{S}$.
- For $\mathbf{x} \in \mathcal{S}$, consider the corresponding parallel curve $\mathcal{C}$. Let $\boldsymbol{T}, \mathbf{N}$ and $\mathbf{B}$ be the Frénet-Serret vectors at $\mathbf{x}$.
- Prescribe the following boundary conditions $\mathbf{x} \in \mathcal{C}$

$$\boldsymbol{n} = \boldsymbol{T},\ \mathbf{m} = \boldsymbol{N},\ \boldsymbol{p} = \mathbf{B},\ \frac{\partial \omega}{\partial \boldsymbol{N}} = q,\ \frac{\partial \vartheta}{\partial \mathbf{B}} = q,$$

Note that $\mathcal{S}$ corresponds to the level surface $\mathcal{S}_{\boldsymbol{p},0}$; in general may not be smooth. It amounts to assuming that the capside is the first level surface: $\mathcal{S}_{\boldsymbol{p},0}$

Energy minimization

Let $\mathcal{B}$ be an axisymmetric domain with flat boundaries at $z = - \pm L$.
Let $0 < c < 1$ be fixed, and suppose that previous model assumptions hold. Either suppose that

1. $\Omega_0 \neq \emptyset$ is prescribed and such that $\Omega = \mathcal{B} - \Omega_0$ is also axisymmetric, with same axis as $\mathcal{B}$, or
2. Ω_0 is the graph of the surface $z = g(r)$, $0 < r < r_0$, with $r = 0$ the axis of the capsid.

Then, there is a minimizer set $\{\boldsymbol{n}, \mathbf{m}, \boldsymbol{p}, \omega, \vartheta\}$ in the admissible (Sobolev) space, and such that $\boldsymbol{n}$ has a discrete number of singular points, that is, $\boldsymbol{n}(\mathbf{x}_k) = \mathbf{0}$.

Consequences

- The singular points $\{\mathbf{x}_k\}$ provide locations of filament crossings between level surfaces.
- The theorem does not specify their locations.
- There are two families of axisymmetric, ordered (layered) level surfaces $\{\mathcal{S}^i_{\mathbf{m}}\}_{i=1}^{M}$ and $\{\mathcal{S}^j_{\boldsymbol{p}}\}_{j=1}^{P}$.
- The family of piecewise smooth, oriented curves

$$\mathcal{C}_{i,j} = \mathcal{S}_{\mathbf{m}i} \cap \mathcal{S}_{\mathbf{p}j},\ 0 \le i \le M,\ 0 \le j \le P,$$

give the location of the DNA axis in the capsid. These are the level curves $\omega(\mathbf{x}) = m_i \quad \vartheta(\mathbf{x}) = p_j$.

Filament reconstitution

Find a piecewise smooth curve, the midline of the filament, $\mathbf{x} = \mathbf{r}(s)$ such that,

$$\begin{aligned} \mathbf{r}'(s) =& \boldsymbol{n}(\mathbf{r}(s)), \quad s \in (0, l_{ij}), \\ & |\boldsymbol{n}| = 1, \\ & \mathbf{r}(0) = \mathbf{r}_0, \end{aligned}$$

where s represents the parameter of the C_{ij}-curve, consisting of the phase fields ω and φ.
$\mathbf{r}_0$ gives the location of the attached filament tip, at the entrance of the capsid. It is prescribed by a protein.
Difficulty:
Note that, as a consequence of the unit director length constraint, $|\mathbf{r}'(s)| = 1$: inextensibility of DNA filament.
Strong experimental evidence opposing this constraint.
Relax constraint $|\boldsymbol{n}| = 1$ adding penalty term $|\boldsymbol{n}(\mathbf{x}) - 1|^2$ in energy.

Testing of the model

Assume capsid as sphere truncated at the poles, with DNA spooled around the distinguished axis, with layering directions arranged in cylindrical symmetry:

$$\boldsymbol{n} = \boldsymbol{e}_\theta, \ \boldsymbol{p} = -\boldsymbol{e}_r, \ \mathbf{m} = \boldsymbol{e}_z$$
$$\nabla\vartheta = q\mathbf{m}, \ \nabla\omega = q\boldsymbol{p}.$$

- Minimize the resulting energy with respect to isotropic core r_c.
- Compare the result obtained by energy minimization with the experimentally determined core radius.

Minimize the resulting energy with respect to the unknown core radius r_c.

Data and Results

The data used in these calculations, scaled with respect to the capsid radius, and the results are given in the next two tables:

Virus	Capsid Radius	DNA length	DNA Conc. c
T4	40.0	55047.60	1.008
T5	42.0	39423.80	0.624
T7	26.05	12932.00	0.857
E15	28.37	12846.00	0.659

Virus	Exp. Core Size	Model Core Size	Percent. Error
T4	0.5500	0.5348	2.76%
*T5	0.4286	0.4268	0.40%
T7	0.5889	0.5712	3.00%
E15	0.5735	0.5699	0.63%

Effect of capside core and shape

For high concentration [Onsager: 1949]:

$$\nu = K_B T \ln(\frac{4}{\pi} c^2 - \frac{45}{8} + c^{-2}) - 1$$

For small concentration [Roij; 2005]:

$$\nu = K_B T \ln \frac{c}{4\pi} + c - 1.$$

Surface tension between ordered and disordered phase [Doi, Kuzuu; 1985]:

$$\sigma = K_B T \frac{0.257}{L_p d}$$

In the calculation of the core radius of virus T5, approximations in the low concentration regime have been used.

Larger errors have been found for viruses with capsid shape strongly departing from spherical and also for capsides with large core.

Gel capsid and ionic model

New dependent fields: Φ, electrostatic potential; $0 < \phi < 1$, DNA volume fraction in capsid; $\{c_i\}_{i=1,\dots Z}$ concentrations of Z ion families with valance z_i; d, interlayer spacing; $\hat{\sigma}(\mathbf{x})$, linear DNA charge density, with imprinted chirality pitch. Energy terms F_{d} accounting for layer compressibility, Flory-Huggins mixing and electric energies, added to mechanical energy:

$$\mathcal{E} = \int_{\Omega} \left(F_{\mathrm{NA}} + F_{\mathrm{d}}\right) d\mathbf{x} + \int_{\mathcal{B}} F_{\mathrm{FH}}(\phi, 1-\phi)\, d\mathbf{x} + \int_{\mathcal{U}} \frac{\bar{\epsilon}}{2} |\nabla \Phi|^2 \, d\mathbf{x} + \nu \mathrm{Vol}(\Omega_0) + \sigma \mathrm{Area}(\partial \Omega_0)$$

Additional constraints and boundary conditions

$$\frac{\epsilon}{2\pi}\triangle\Phi = -\chi_{\mathcal{B}}\frac{\pi\hat{\sigma}d^2}{4} + \sum_{i=1}^{N} z_i c_i \ \text{ in } \mathcal{U} = \mathcal{B}\cup\mathcal{B}_{\text{ext}}$$

$$[\epsilon\frac{\partial\Phi}{\partial\nu}] = 0 \text{ on } \partial\mathcal{B}, \ \ \frac{\partial\Phi}{\partial\nu} = 0 \text{ on } \partial\mathcal{U}.$$

Local form of conservation of mass of DNA:

$$\gamma_{\text{dna}} d^2(r(s))\phi(\mathbf{r}(s))|\mathbf{r}'(s)| = m_0.$$

m_0: total mass of the DNA: γ_{dna}, reference density

Permeability of the capsid-allowing for transport of water and ions across- requires appropriate boundary conditions [Yao, MCC, Mori; 2014, 2015], [Yao, MCC, Siegel, Mori; 2017], [Chabaud, MCC; 2016], [MCC, Golovaty, Lavrentovich, Walkington; 2016]

Conclusions

We have developed a liquid crystal based model combining tools from smectic and chromonic liquid crystals. Application of Hamilton's variational approach yields a time dependent model with inertia.

Conclusions

We have developed a liquid crystal based model combining tools from smectic and chromonic liquid crystals. Application of Hamilton's variational approach yields a time dependent model with inertia.

- Adjust lyotropic funcions (smectic energy coefficient, isotropic energy density, surface thension) from experiments that prescribe partial genome lenghts of a give virus.
- Calculate pressures predicted by the system: this requires including the electric properties in the model.
- Map observed DNA kinks and knots to model predictions.
- Calculate shearing stress and make predictions on ejection speeds.
- Use pressure and shearing stress measuremts to adjust remaining parameters of the model.
- Numerical simulations of realistic capsid shapes and make predictions for our laboratory synthesized viruses.